Eur. Phys. J. A **17**, 349–355 (2003)
DOI 10.1140/epja/i2002-10176-7

THE EUROPEAN PHYSICAL JOURNAL A

Deviation of the nucleon shape from spherical symmetry: Experimental status

A.M. Bernstein[a]

MIT, Laboratory for Nuclear Science, Cambridge, MA 02139, USA

Received: 1 November 2002 /
Published online: 15 July 2003 –

Abstract. In this brief pedagogical overview the physical basis of the deviation of the nucleon shape from spherical symmetry will be presented along with the experimental methods used to determine it by the $\gamma^* p \rightarrow \Delta$ reaction. The fact that non-spherical electric ($E2$) and Coulomb quadrupole ($C2$) amplitudes have been observed will be demonstrated. We have measured these multipoles for the N, Δ system as a function of Q^2 from the photon point through 4 GeV^2 with modest precision. Their precise magnitude remains model dependent due to the contributions of the background amplitudes, although rapid progress is being made to reduce these uncertainties. A discussion of what is required to perform a model-independent analysis is presented. All of the data to date are consistent with an oblate shape for the proton and a prolate shape for the Δ.

PACS. 13.60.Le Meson production – 13.88.+e Polarization in interactions and scattering – 13.40.Gp Electromagnetic form factors – 14.20.Gk Baryon resonances with $S = 0$

1 Introduction

Experimental confirmation of the deviation of the proton structure from spherical symmetry is fundamental and has been the subject of intense experimental and theoretical interest [1] since this possibility was originally raised by Glashow [2]. The most direct method to determine this would be to measure the quadrupole moment of the proton. However since the proton spin is 1/2, this is not possible. Therefore, this determination has focused on the measurement of the electric and Coulomb quadrupole amplitudes ($E2$, $C2$) in the predominantly $M1$ (magnetic dipole-quark spin flip) $\gamma^* N \rightarrow \Delta(1/2 \rightarrow 3/2)$ transition. Thus, measurements of the $E2$ and $C2$ amplitudes represent deviations from spherical symmetry of the N, Δ system and not the nucleon alone. The experimental difficulty is that the $E2/M1$ and $C2/M1$ ratios are small (typically $\simeq -2$ to -8 % at low Q^2). In this case the non-resonant (background) and resonant quadrupole amplitudes are of the same order of magnitude. Therefore, experiments have to be designed to attain the required precision to separate the signal and background contributions. This has been accomplished for photo-pion reactions for the $E2$ amplitude using polarized photon beams [3,4]. In pion electroproduction the deviation from spherical symmetry is easier to observe due to the interference between the longitudinal (Coulomb) $C2$ and the dominant $M1$ amplitudes by observation of the σ_{TL} cross-section [5]. Electroproduction experiments are also being performed for a range of four momenta Q^2 which provides a measure of the spatial distribution of the transition densities. On the other hand, the presence of the additional longitudinal multipoles in electroproduction means that there are more observables to measure and therefore more data must be taken than in photoproduction experiments. The experiments to generate an extensive data-base that would allow a model-independent analysis have just begun. At the present time one must rely on reaction models to extract the resonant $M1$, $E2$, and $C2$ amplitudes of interest from the data. As has been pointed out the model error can be much larger than the experimental error [5]. Therefore, it is important to test model calculations for a range of center-of-mass (CM) energies W in the region of 1232 MeV, the resonant energy, which provides a range of the relative background and resonant amplitudes, as well as picking out specific observables which are sensitive to the quadrupole amplitudes (*e.g.*, σ_{TL}) and others which are primarily sensitive to the background amplitudes (*e.g.*, $\sigma_{TL'}$).

2 Why should the nucleon be deformed?

It is well known that in the quark model there are non-central (tensor) interactions between quarks which were modeled after the electromagnetic interaction [2,6].

[a] e-mail: bernstein@mitlns.mit.edu

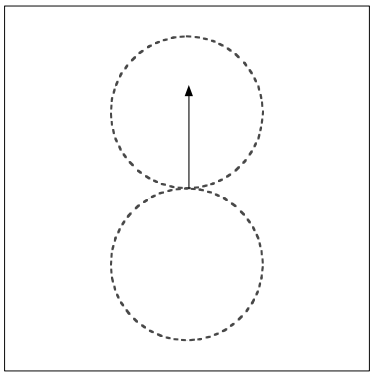

Fig. 1. The pion cloud contribution to nucleon structure. The arrow represents the nucleon spin vector and the dashed line the pion cloud.

Although this interaction does, in fact, introduce non-spherical responses ($E2$ and $C2$) into the electromagnetic matrix elements, they are only approximately 10% of the observed amplitudes. In my view this is not surprising since the long-distance part of the nucleon and Δ structure should be related to the pion cloud which is poorly represented in quark models. We expect the long-range (low Q^2) behavior to be pion field dominated since it is the lightest hadron. This of course is well known experimentally and is a cornerstone of classical nuclear theory, What is new in our more recent understanding is that the pion itself, and its interaction with other hadrons, is a consequence of spontaneous chiral-symmetry breaking in QCD [7]. In the chiral limit, *i.e.* where the light quark masses are set equal to zero, the QCD Lagrangian has chiral symmetry which does not appear in nature. We know this experimentally since if chiral symmetry were exact, we would observe parity doubling of all hadronic states. This means that the chiral symmetry is broken (or more exactly hidden) and is manifested in the appearance of zero-mass, pseudoscalar Goldstone bosons. Since, in nature, the light quark masses are small but non-zero, the physical Goldstone bosons have a small mass and are identified as the π-mesons. The coupling of a Goldstone boson to a nucleon is $g\boldsymbol{\sigma}\cdot\mathbf{p}$, where g is the πN coupling constant (predicted by the Goldberger-Trieman relation), σ is the nucleon spin, and p is the pion momentum. This interaction vanishes in the s wave and leads to the Goldstone theorem that the interaction vanishes as $p \to 0$. The $\boldsymbol{\sigma}\cdot\mathbf{p}$ interaction is strong in the p wave which leads to the Δ-resonance and is the basis of the deviation from spherical symmetry in the nucleon (illustrated schematically in fig. 1) and Δ structure. In a sense, this is the basis of classical nuclear theory.

Although it is beyond the scope of this presentation, I cannot resist mentioning that the $\boldsymbol{\sigma}\cdot\mathbf{p}$ interaction required by the spontaneous breakdown of chiral symmetry in QCD, economically describes the basics of πN scattering and of nuclear physics. Indeed, this πN interaction leads to a non-spherical NN interaction (the tensor force). By generalizing fig. 1 to the case of two nucleons, it is not hard to see physically (semi-classically) that the most attractive position for two nucleons is for one nucleon to be spatially above the second with their spins parallel. This is the configuration which is favored by the tensor force.

Table 1. Experimental and model amplitudes for the $\gamma N \to \Delta$ reaction. The units for $M1$ and $E2$ are 10^{-3} GeV$^{-1/2}$ and $E2/M1$ in %. The numbers in parentheses are experimental errors.

Model	$M1$	$E2$	$E2/M1$
Experiment [8]	288(8)	−7.2(0.5)	−2.5(0.5)
QM: Capstick [9]	196	−0.1	−0.04
QM: Buchmann [10]	203	−7.0	−3.5
SL (bare) [11]	175	−2.2	−1.2
SL (dressed) [11]	257	−6.8	−2.7

Quantitatively the quark model calculations of the $M1$ matrix element are well known to be too small (although not often discussed) [9]. This is shown in table 1, where the magnitude of the experimental [8] and theoretical matrix elements for the $\gamma N \to \Delta$ reaction are presented. It can be seen that the quark model predictions are $\simeq 30\%$ too low for the dominant magnetic dipole ($M1$) and an order of magnitude too small for the $E2$ matrix element, which is the indicator of the non-spherical structure of the nucleon and Δ structure. The table also includes the redundant $E2/M1$ ratio just to illustrate that it has become commonplace in the recent literature to quote only this latter ratio and not the absolute values of the matrix elements. By doing so, some important lessons tend to be overlooked. As an example, we focus on the quark model extensions of Buchmann and collaborators [10], which introduce multi-body interactions between the quarks, taking into account the composite nature of the constituent quarks. These currents take the pion field partially into account and as can be seen in table 1, this effect increases the $E2$ matrix element to the empirical size and in fact increases the $E2/M1$ ratio to an even larger value than the experiment. However, this treatment does not increase the magnitude of the $M1$ matrix element so it remains $\simeq 30\%$ less than experiment. As was discussed above, based on spontaneous chiral-symmetry breaking, it is physically intuitive that this shortfall should be looked for in the long-range effect of the pion cloud.

This issue of the quark core and pion cloud contributions has been addressed in a meson exchange model which is based on the picture of spontaneous chiral-symmetry breaking by Sato and Lee [11]. Their model results are also presented in table 1. Here, it is seen that their model quantitatively makes up for the deficiencies of the quark model, not only for the $E2/M1$ ratio, but for the individual magnitudes of the $E2$ and $M1$ matrix elements. Sato and Lee have also calculated the effects of the pion cloud for pion electroproduction as a function of Q^2 and the results are presented in fig. 2. It can be seen that the enhancement of the $M1$ matrix element is significant and that the non-spherical $E2$ and $C2$ (Coulomb quadrupole) matrix elements are dominated by meson cloud effects. It is also seen in fig. 2 that, as expected, the long-range pion

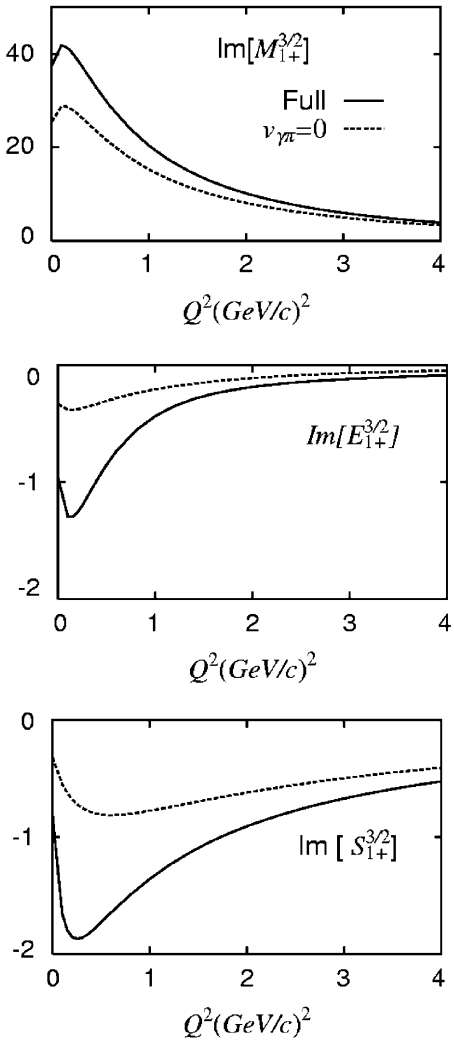

Fig. 2. The contribution of the quarks and pion cloud to the $M1$, $C2$, and $E2$ transition amplitudes in the $\gamma^* p \to \Delta$ reaction calculated by Sato and Lee [11].

cloud effects are more dominant at low Q^2. The dynamic Sato-Lee calculations are in excellent agreement with the data for photo-pion production in the Δ region (some of the parameters were fit to these data) and are also in good agreement with the JLab data presented by Burkert (this issue, p. 303). However, before becoming complacent, we should note that the next section will show that this model is not in agreement with low-Q^2 data taken at Bates [5, 12] near the predicted peak of the pion cloud contribution.

The question of the shape of the nucleon and Δ were explored in the context of three different models by Buchmann and Henley [13]. They conclude that the proton is prolate (longer at the poles) and the Δ is oblate (flatter at the poles). This is consistent with the data [4].

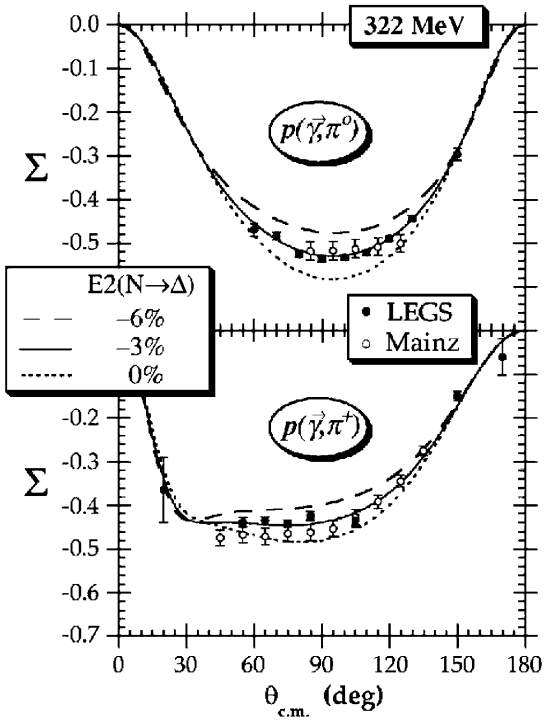

Fig. 3. Polarized-photon asymmetries for the $\gamma p \to \pi^0 p$ and $\gamma p \to \pi^+ n$ reactions plotted *versus* θ. The curves are MAID [14] for different $E2/M1$ ratios as shown.

3 Experiments on proton deformation

Modern photon experiments have been carried out at Mainz [3] and Brookhaven [4] of the $\gamma p \to \pi^0 p$ and $\gamma p \to \pi^+ n$ reactions with polarized photons. The combination of accurate measurements and the use of polarized photons provides sufficient sensitivity to obtain both the small $E2$ amplitude and the dominant $M1$ amplitude. The measurement of both charge channels allows an isospin separation of the resonant $I = 3/2$ channel. The results for the polarized-photon asymmetry are presented in fig. 3. There is good agreement for this quantity between the two labs and model calculations and the results are $E2/M1 = -2.5 \pm 0.5\%$ [8] showing that there is significant deformation in the N, Δ system. It should be mentioned, however, that although there is very good agreement between the Mainz and Brookhaven measurements of the polarized-photon asymmetries shown in fig. 3, there is a significant deviation in the unpolarized cross-sections [3, 4] which, unfortunately, is still unresolved.

The situation for pion electroproduction in the Δ-resonance region is evolving rapidly with activity at all the intermediate-energy facilities Bates, Bonn, JLab, and Mainz (for a review, see [1]). In this brief report only a few highlights will be mentioned. The work at Bates will be emphasized here since the focus on this talk is on the pion cloud effects which are largest in the low-Q^2 regime covered by those experiments and also since the JLab work was covered by Burkert (this issue, p. 303). There has been a corresponding increase in the theoretical activity in this field which is being emphasized in a complementary talk

by Tiator (this issue, p. 357) who also presents an overview of the data. The goal of the pion electroproduction experiments is to obtain accurate data which has sufficient sensitivity to determine the $M1$, $E2$, and $C2$ resonance amplitudes, but also sufficient coverage to determine the background amplitudes which are of the same order of magnitude as $E2$ and $C2$. These are of interest in their own right as an integral part of the $\gamma\pi N$ system and therefore as part of the chiral structure of matter. For example, the resonance and background amplitudes are related to the form factors and to the electric and magnetic polarizabilities of the nucleon. The background amplitudes contribute to the cross-sections linearly with the resonance amplitudes, and the interference terms therefore make significant contributions to the observables. The background contributions also occur in the resonance amplitudes and are part of the physics. In a sense this is a crucial difference between dynamics and static models for which the Δ is treated as a bound state (which ignores the background contributions). The cleanest experimental determination would consist of an empirical multipole analysis of the data. At the present time we do not have a sufficient, accurate data-base with which to perform such an analysis and must rely on empirical models to extract the resonant amplitudes. The present short-term experimental goal is to provide a sufficiently sensitive and accurate data-base to rigorously test the models. It is hoped that the combination of Born terms and the tails of higher resonances will suffice to reproduce the background amplitudes.

The coincident $p(\mathbf{e}, e'\pi)$ cross-section in the one-photon exchange approximation can be written as [15]:

$$\frac{\mathrm{d}\sigma}{\mathrm{d}\omega \mathrm{d}\Omega_e \mathrm{d}\Omega_\pi^{\mathrm{cm}}} = \Gamma_{\mathrm{v}}\ \sigma_h(\theta,\phi)\,, \tag{1}$$

$$\sigma_h(\theta,\phi) = \sigma_T + \varepsilon\sigma_L + \sqrt{2\varepsilon(1+\varepsilon)}\sigma_{TL}\cos\phi\,, \\ +\varepsilon\sigma_{TT}\cos 2\phi + hp_e\sqrt{2\varepsilon(1-\varepsilon)}\sigma_{TL'}\,,$$

where Γ_{v} is the virtual photon flux, $h = \pm 1$ is the electron helicity, p_e is the magnitude of the longitudinal electron polarization, ε is the virtual photon polarization, θ and ϕ are the pion CM polar and azimuthal angles relative to the momentum transfer $\mathbf{q}$, and σ_L, σ_T, σ_{TL}, and σ_{TT} are the longitudinal, transverse, transverse-longitudinal, and transverse-transverse interference cross-sections, respectively. Each of these partial cross-sections can be written in terms of the multipoles [15]. The $E2$ and $M1$ amplitudes can be obtained from a combination of σ_T and σ_{TT} as was done in photo-production (the polarized-photon asymmetry $= \sigma_{TT}/\sigma_T$). In the approximation that only s and p wave pions are produced they can be written as [15]:

$$\sigma_T(\theta) = A_T + B_T\cos\theta + C_T\cos^2\theta\,, \tag{2}$$
$$\sigma_{TT}(\theta) = \sin^2\theta A_{TT}\,,$$
$$A_T \approx 5/2|M_{1+}|^2 + \mathrm{Re}[M_{1+}M_{1-}^* - 3M_{1+}E_{1+}^*]\,,$$
$$B_T \approx 2M_{1+}E_{0+}^*\,,$$
$$C_T \approx -3/2|M_{1+}|^2 + \mathrm{Re}[9M_{1+}E_{1+}^* - 3M_{1+}M_{1-}^*]\,,$$
$$A_{TT} \approx -1/2|M_{1+}|^2 - \mathrm{Re}[M_{1+}E_{1+}^* + M_{1+}M_{1-}^*]\,,$$

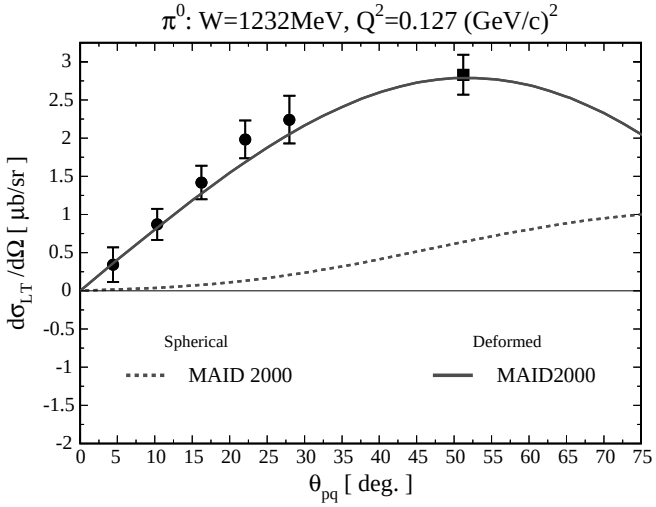

Fig. 4. The differential cross-section for the $ep \to e'\pi^0 p$ reaction plotted *versus* θ_{pq}, the CM angle of the proton relative to the momentum transfer $\mathbf{q}$ (the pion CM angle $= 180^0 - \theta_{pq}$) [5, 12]. The curves are from the MAID model [14] with and without the $C2$ contribution.

where the pion production multipole amplitudes are denoted by $M_{l\pm}$, $E_{l\pm}$, and $L_{l\pm}$, indicating their character (magnetic, electric, or longitudinal), and their total angular momentum ($J = l \pm 1/2$). The expressions for A_T, B_T, C_T and A_{TT} are in the truncated multipole approximation, where it is assumed that only terms which interfere with the dominant magnetic dipole amplitude M_{1+} are kept. The exact formulas without this approximation can be found in [15]. In this approximation the longitudinal cross-section $\sigma_L = 0$. In model calculations [11,14,16–18] this approximation is not made and significant deviations from the truncated multipole approximation occur.

The $C2$ amplitude can be obtained from σ_{TL}. An example of this is presented in fig. 4 which shows the Bates data [5] and the difference between the cross-section with and without the quadrupole $C2$ amplitude calculated with the MAID model [14]. The sensitivity is quite large, again indicating a significant d state component in the N, Δ system. As can be seen from a comparison of figs. 3 and 4, there is far more sensitivity to the $C2$ as compared to the $E2$ amplitude, despite the fact that they are both only a few % of the $M1$ amplitude. The reason for this difference lies in the fact that in the longitudinal amplitude the $C2$ is a leading term, whereas in the transverse amplitude the $E2$ occurs in a linear combination with the $M1$ amplitude.

The TL' and the TL (transverse-longitudinal) response functions are the real and imaginary parts of the same combination of interference multipole amplitudes. Again assuming that only s and p wave pions are produced they can be written as [15]

$$\sigma_{TL}(\theta) = -\sin\theta\mathrm{Re}[A_{TL} + B_{TL}\cos\theta]\,, \tag{3}$$
$$\sigma_{TL'}(\theta) = \sin\theta\mathrm{Im}[A_{TL} + B_{TL}\cos\theta]\,,$$
$$A_{TL} \approx -L_{0+}^* M_{1+}\,,$$
$$B_{TL} \approx -6L_{1+}^* M_{1+}\,,$$

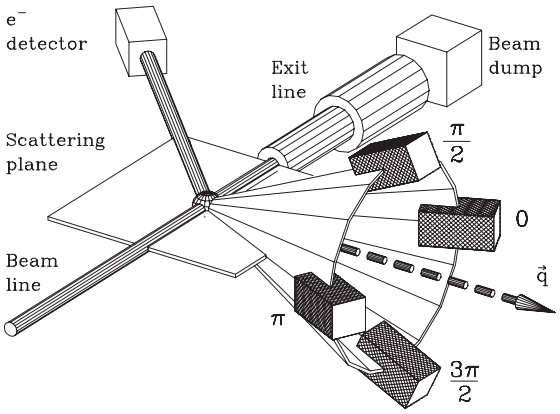

Fig. 5. A schematic diagram of the out-of-plane spectrometer system (OOPS) at Bates. See text for discussion.

where the last two approximations are for the truncated multipole approximation.

The Bates out-of-plane spectrometer system [19] which was designed and built in order to exploit the ϕ-dependence shown in eq. (2), is shown schematically in fig. 5. It consists of an electron spectrometer used in conjunction with four relatively light spectrometers which can be deployed at a fixed polar angle θ_{hq}, relative to the momentum transfer $\mathbf{q}$ to detect the charged, emitted hadron (p, π^+). By deploying multiple (3 or 4) spectrometers at different azimuthal angles ϕ, the combination of $\sigma_0 = \sigma_T + \epsilon\sigma_L, \sigma_{TT}$ and σ_{TL} can be simultaneously measured in one run which reduces the systematic errors caused by luminosity measurement errors. Furthermore, the geometry is optimized to measure relatively small relative magnitudes of σ_{TL}/σ_0 and σ_{TT}/σ_0. The combination of high luminosity and small systematic errors, allow precise measurements to be performed. Furthermore, when polarized electron beams are employed, measurements of the fifth structure function $\sigma_{TL'}$, which require out-of-plane hadron detection, become possible.

Several rounds of experiments have been carried out at Bates with the OOPS apparatus [5,12]. Experiments have been carried out at $Q^2 = 0.127$ GeV^2 over a range of CM energies W, below, on, and above the Δ-resonance energy $W = 1232$ MeV. For brevity only the results at the Δ peak are presented in fig. 6. The experimental results are compared to calculations [11,14,16–18]. The most ambitious calculations are the dynamical Sato-Lee model [11] and a dispersion relation calculation [17]. The Sato-Lee model calculates all of the multipoles and πN scattering from dynamical equations. Dispersion relation calculations have previously provided good agreement with photo-pion production data [20]. Unfortunately, neither of these calculations agrees with the Bates data. The Sato-Lee model [11] agrees for the unpolarized cross-sections $\sigma_0 = \sigma_T + \epsilon\sigma_L$ but is in strong disagreement with the measurements of σ_{TL} and $\sigma_{TL'}$. The dispersion relations calculation [17] agrees with some of the Bates data but disagrees with the measurement of σ_0 at $W = 1170$ MeV (not shown here) and with σ_{TL} measurements. Only the two most empirical models [14,18] give reasonable overall fits to all of the

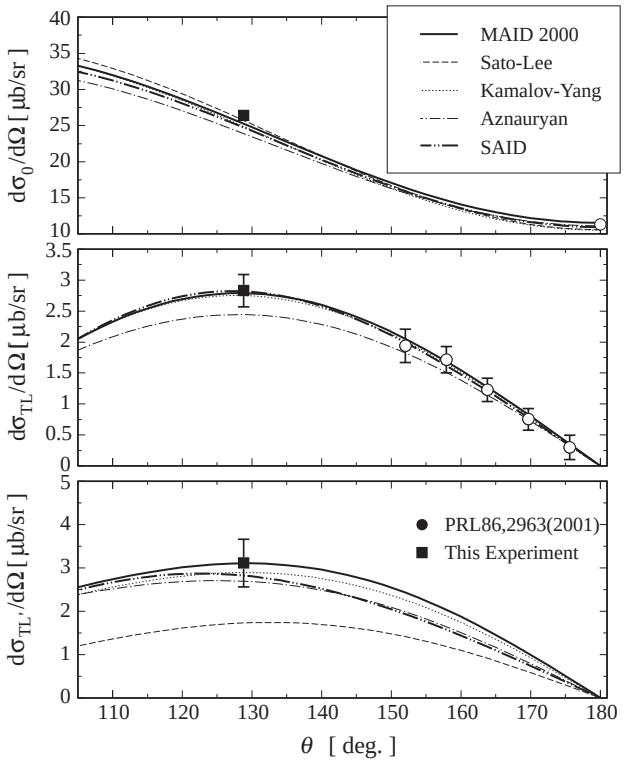

Fig. 6. Cross-sections for the $p(\mathbf{e}, e'p)\pi^0$ reaction for $W = 1232$ MeV, $Q^2 = 0.127$ (GeV/c)^2 plotted *versus* θ. The top panel is for $\sigma_0 = \sigma_T + \epsilon\sigma_L$. The middle panel is for σ_{TL} and the bottom panel is for $\sigma_{TL'}$. The curves are MAID [14] (solid line), Sato-Lee [11] (dashed line), Kamalov *et al.* [16] (dotted line), dispersion theory [17] (dot-dashed line), and empirical multipole fit to previous pion electroproduction data (SAID) [18] (long-dashed line).

Bates data. The Mainz Unitary Model (MAID) is a flexible way to fit observed cross-sections as a function of Q^2 [14]. It incorporates Breit-Wigner resonant terms, Born terms, higher N^*-resonances, and is unitarized using empirical πN phase shifts. The fitted parameters of the model include a range of data [14]. The SAID calculation [18] is an empirical multipole fit to previous electropion production data. The Kamalov-Yang model [16] includes dynamics for the resonant channels and uses the background amplitudes of the MAID model. This model is in reasonable agreement with most of the Bates data with the exception of the unpolarized cross-section σ_0 at $W = 1170$ MeV (not shown here).

The Sato-Lee dynamical model [11] predicts that the pion cloud is the dominant contribution to the quadrupole amplitudes at low values of Q^2. Unfortunately, this model is not in agreement with our data but showed much better predictions of the recently reported result from the CLAS detector at JLab for the $p(\mathbf{e}, e'p)\pi^0$ reaction in the Δ region for Q^2 from 0.4 to 1.8 (GeV/c)^2 [21]. This seems to indicate that the dominant meson cloud contribution, which is predicted to be a maximum near our values of Q^2, is not quantitatively correct. This suggests to me that they are not completely implementing the dynamics of chiral-symmetry breaking, perhaps in their treatment of the pion

loops which are required in chiral perturbation theory calculations of the near-threshold $ep \to e\pi^0 p$ reaction.

Recently, a measurement of $A_{TL'}$ for the $p(\mathbf{e}, e'p)\pi^0$ reaction in the Δ region was performed at Mainz [22]. The kinematics include a range of Q^2 values from 0.17 to 0.26 $(\mathrm{GeV}/c)^2$ and backward θ-angles. These data were compared to several models [11,14,16] which all disagreed with the data. The results of the MAID calculation had to be multiplied by 0.75 to agree with the experiment [22]. In comparison with the Bates $\sigma_{TL'}$ data [12], if one multiplies the MAID results by the same factor these data are still in agreement at $W = 1170$ MeV and at $W = 1232$ MeV they do not agree with a discrepancy of 1.4σ. Therefore, a reduction of 25% in the MAID predictions for $\sigma_{TL'}$ does not seriously effect the agreement with the Bates experiment.

It is of interest to compare the TL and TL' results presented here with those of the recoil polarizations which are proportional to the real and imaginary parts of interference multipole amplitudes. For the $p(\mathbf{e}, e'\mathbf{p})\pi^0$ channel the outgoing-proton polarizations have been observed in parallel kinematics (the protons emitted along $\mathbf{q}$ or $\theta = 180^\circ$) [23,24]. For this case the observable amplitudes are [15]:

$$\begin{aligned} \sigma_0\, p_x &\propto \mathrm{Re}[A^x_{TL}]\,, \\ \sigma_0\, p_y &\propto \mathrm{Im}[B^y_{TL}]\,, \\ \sigma_0\, p_z &\propto \mathrm{Re}[C^z_{TT}]\,, \\ A^x_{TL} \approx B^y_{TL} &\approx (4L^*_{1+} - L^*_{0+} + L^*_{1-})M_{1+}\,, \\ C^z_{TT} &\approx \mid M_{1+} \mid^2 + \mathrm{Re}[(6E^*_{1+} - 2E^*_{0+})M_{1+}]\,, \end{aligned} \tag{4}$$

where σ_0 is the unpolarized cross-section and the constants of proportionality contain only kinematic factors. The formulas for $A^x_{TL}, B^y_{TL}, C^z_{TT}$ assume s and p wave pions are produced and are in the truncated multipole approximation. This shows both the similarity and detailed difference between a measurement of TL and TL' and the recoil polarizations. In the published papers the data were compared to the MAID model which is not in good agreement with the data [23,24]. At the present time we do not have sufficient data to pin down the multipoles which are responsible for this difference.

Experiments at Bonn [1] and JLab [21] have measured the $\gamma^* p \to \Delta$ reaction over a wide range of Q^2 values. The data have been analyzed with a variety of methods including the truncated multipole approximation and the MAID [14] and SAID [18] models. The results have provided us with a consistent overall picture of the EMR and CMR ratios as a function of Q^2 which was presented by Burkert (this issue, p. 303). It is seen that the pion cloud models [11,16] are in reasonable agreement with the data for $Q^2 \geq 0.4$ GeV^2. For lower values of Q^2, near the peak of the pion cloud contribution, as measured at Bates and Mainz, they are only in qualitative agreement.

It is interesting to consider how much data is required to perform a complete, model-independent, multipole analysis. This can be illustrated in the approximation where it is assumed that only s and p wave pions are emitted (the discussion can be easily generalized without this assumption). In this case there are 8 multipoles for electroproduction $(E_{0+}, E_{1\pm}, M_{1\pm}, L_{0+}, L_{1\pm})$. Since these are complex they represent 16 numbers. However, an overall phase is irrelevant, so this leaves 15 numbers to be determined at each value of Q^2 and W. By counting the observables in eqs. (2) and (3) it can be seen that for polarized electrons and unpolarized targets there are 8 observables, namely A, B, C, A_{TT}, Re$[A_{TL}]$, Im$[A_{TL}]$, Re$[B_{TL}]$, Im$[B_{TL}]$ in eqs. (2) and (3).This is the number we have obtained at Bates (including data presently being analyzed) at $Q^2 = 0.127$ GeV^2. By adding recoil polarization observables in parallel kinematics, 3 more numbers are measured (eq. (4)). This provides a stringent test of the reaction models but not enough to make a model-independent analysis. By measuring recoil polarization away from the forward direction the remainder can be measured. It is of interest to compare this to the photon experiments which have been carried out with polarized photons and unpolarized targets. There are 5 transverse multipoles which makes $10 - 1 = 9$ numbers to determine. The actual experiments [3,4] determined 4 of these (A, B, C and A_{TT} of eq. (2)). So even these data are not yet sufficient for a model-independent analysis, and polarized target data is required to complete this task. Such experiments are underway at LEGS in Brookhaven and are being planned at Mainz.

In conclusion, we have definitively observed the deviation of the nucleon and Δ from spherical symmetry. We are making rapid progress towards making a quantitative measurement of this effect. The errors are primarily in the model extraction of the deformation. We are also making rapid progress towards stringently testing the reaction models, which means pinning down the background amplitudes. This consists of measurements of the fifth structure function $\sigma_{TL'}$ and of the recoil polarizations. In addition, we are also making progress towards a sufficient data-base to approach making model-independent analyses.

References

1. See, *e.g.*, *NStar 2001, Proceedings of the Workshop on the Physics of Excited Nucleons*, edited by D. Drechsel, L. Tiator (World Scientific, Singapore, 2001).
2. S.L. Glashow, Physica A **96**, 27 (1979).
3. R. Beck *et al.*, Phys. Rev. C **61**, 35204 (2000).
4. G. Blanpied *et al.*, Phys. Rev. C **64**, 025203 (2001).
5. C. Mertz *et al.*, Phys. Rev. Lett. **86**, 2963 (2001).
6. N. Isgur, G. Karl, R. Koniuk, Phys. Rev. D **25**, 2394 (1982).
7. For an introduction to chiral-symmetry breaking in QCD and a review of this field see, *e.g.*, *Chiral Dynamics 2000: Theory and Experiment*, edited by A.M. Bernstein, J.L. Goity, U.G. Meißner (World Scientific, Singapore, 2001).
8. Particle Data Group (K. Hagiwara *et al.*), *Review of Particle Physics*, Phys. Rev. D **66**, 010001 (2002).
9. S. Capstick, Phys. Rev. D **46**, 1965 (1992).
10. A.J. Buchmann, E. Hernandez, A. Faessler, Phys. Rev. C **55**, 1 (1997).

11. T. Sato, T.-S.H. Lee, Phys. Rev. C **63**, 055201 (2001).
12. C. Kunz *et al.*, in preparation; C. Kunz, PhD Thesis, MIT (2000); C. Vellidis, PhD Thesis, University of Athens (2001).
13. A.J. Buchmann, E.M. Henley, Phys. Rev. C **63**, 015202 (2000).
14. D. Drechsel *et al.*, Nucl. Phys. A **645**, 145 (1999) and `http://www.kph.uni-mainz.de/MAID/`.
15. D. Drechsel, L. Tiator, J. Phys. G **18**, 449 (1992); A.S. Raskin, T.W. Donnelly, Ann. Phys. (N.Y.) **191**, 78 (1989).
16. S.S. Kamalov, S.N. Yang, Phys. Rev. Lett. **83**, 4494 (1999).
17. I.G. Aznauryan, Phys. Rev. D **57**, 2727 (1998) and private communications.
18. R.A. Arndt, I.I. Strakovsky, R.L. Workman, nucl-th/0110001 and `http://gwdac.phys.gwu.edu`. The current, N217, solution is presented here.
19. S.M. Dolfini *et al.*, Nucl. Instrum. Methods A **344**, 571 (1994); J. Mandeville *et al.*, Nucl. Instrum. Methods A **344**, 583 (1994); Z.-L. Zhou *et al.*, Nucl. Instrum. Methods A **487**, 365 (2002).
20. O. Hanstein, D. Drechsel, L. Tiator Nucl. Phys. A **632**, 561 (1998).
21. K. Joo *et al.*, Phys. Rev. Lett. **88**, 122001 (2002).
22. P. Bartsch *et al.*, Phys. Rev. Lett. **88**, 142001 (2002).
23. G.A. Warren *et al.*, Phys. Rev. C **58**, 3722 (1998).
24. Th. Popischil *et al.*, Phys. Rev. Lett. **86**, 2959 (2001).